Magnetic Near-field Probe for GHz band and Spatial Resolution Improvement Technique

Hiroki Funato,   Takashi Suga

Electronics Development and Design Section, Production Engineering Research Laboratory, Hitachi Ltd.

292 Yoshida-cho, Totsuka-ku, Yokohama, 244-0817 Japan

funato.hiroki@gm.perl.hitachi.co.jp, suga.takashi@gm.perl.hitachi.co.jp

Abstract — **This paper reports magnetic near-field probe for high frequency band up to 10 GHz and novel measurement technique for improvement of spatial resolution. We fabricated two types of magnetic near-field probe and evaluated frequency characteristics for magnetic and electric near-field in isolation. For the measurement results, we proposed accurate equivalent circuit of probes and evaluated each value of lumped parameter to study the difference of probes. Theoretical results accorded with measurement results. With use of fabricated probe, measurement technique for improvement of spatial resolution was proposed. This technique allows improving and easy modification of spatial resolution without redesign of probe.**

I. INTRODUCTION

In order to locate source of electromagnetic radiation or to predict far-field emission level, magnetic near-field measurement is crucial method [1-4]. Today with the dissemination of wireless devices as represented by cell phone or PC with built-in wireless LAN, these wireless modules sometimes cause electromagnetic interference with other digital circuit modules in self equipment [5]. Magnetic near-field measurement is useful to specify the electromagnetic interference paths for those kinds of problems. However the levels of electromagnetic fields in the self-interference problem is much smaller up to several tens of dB than that in excess over regulation problems and it's desired that loop type probes for magnetic field have large loop area as much as possible to improve signal-to-noise ratio. While loop antenna should be posited close to measuring target to improve spatial resolution, but the approaching of probe which has some size causes degradation of measurement accuracy because of induced voltage by electric near-field as noise.

Firstly this report describes that fabrication of two types of magnetic near-field loop probes which has different structure of transmission line and loop element. We estimated frequency characteristics of the probes for electric and magnetic near-field in isolation. Secondly, lumped parameter equivalent circuit was proposed to analyze difference between probes. The circuit has simplified model of loop element. Parameters of the circuit were evaluated and compared measurement results and theoretical results.

II. PROBE AND SETUP

Fig.1 shows structure and sizes of fabricated magnetic near-field probes. Type A has bare loop and Type B has strip line loop other than a side. Both characteristic impedance of transmission line is 50Ω and 15mm Length. The probes have 1 square millimeter loop area as shown in fig.1 and fabricated by standard PCB process by using FR-4.
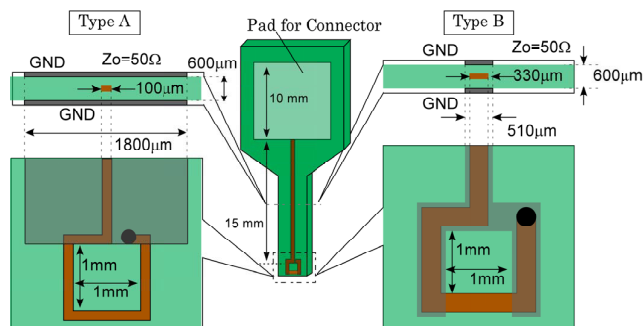

Fig. 1.   Schematic diagram of fabricated magnetic near-field probes (Left: Type A, Right: Type B)
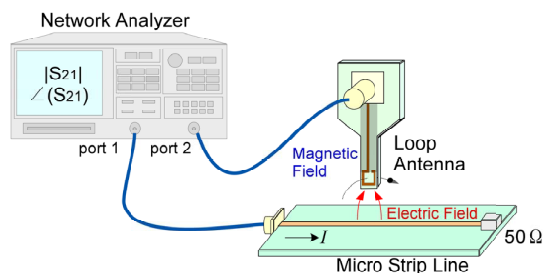

Fig. 2.   Measurement setup for frequency characteristics of S21 parameter of fabricated probes.

To estimate frequency characteristics of probes, we set Micro Strip Line (MSL) as target that has 500μm width copper straight pattern and enough wide GND. Absolute and Phase value of S21 was measured with setting probe close to MSL in frequency 45MHz to 10GHz. Induced voltage by electric near-field and magnetic near-field was separated by add and subtract of vector of S21 with turning probe 0° and 180° at same positions [6]. Height of loop probe type A was set to 1.5 mm and height of loop probe type B was set as that induced voltage by magnetic field was same as it of type A.
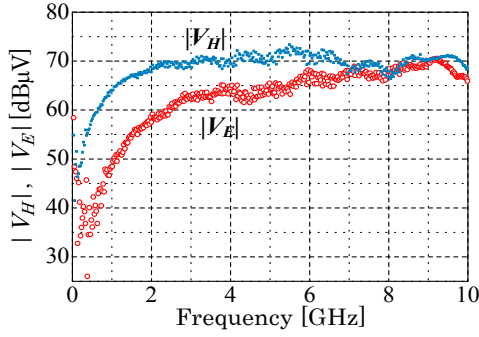
Fig. 3.   Frequency characteristics of induced voltage $|V_H|$ and $|V_E|$ for type A
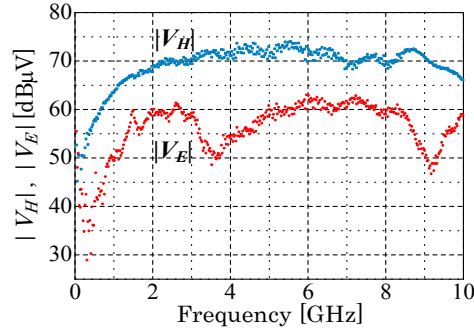
Fig. 4.   Frequency characteristics of induced voltage $|V_H|$ and $|V_E|$ for type B

Frequency characteristics of induced voltage by electric near-field (V_E) and magnetic near-field (V_H) of probe type A are shown in Fig. 3. Both V_E and V_H were calculated from S21 and 0 dBm: source power of network analyzer. V_E is increases and becomes equal with V_H over 6 GHz. Fig.4 shows V_E and V_H of probe type B. In the fig.4, we found resonant points in V_E at 3.5 GHz and 9 GHz and those are originated with the probe structure. As a result, V_E were suppressed up to 10dB than V_H in all band. This result indicates that resonant frequency of common mode impedance of probe is essential for reduction of V_E.

III. EQUIVALENT CIRCUIT ANALYSIS

We proposed lumped parameter equivalent circuit model including measurement setup as shown in Fig.5. Influence of electric near-field is described as capacitive coupling which expresses that electrical flux line between patterns with probe. Transmission line is represented as 8 steps of ladder circuit that satisfy under tithe of minimum wavelength for a step.

The Values of lumped parameter shown in fig.6 was determined by realistic simulation using method of moment. Capacitance $C1$, $C2$,,, Cn which represents as effect of electric near-field and inductance of loop element Lls, $Llg1$, $Llg2$,,, $Llgn$ was evaluated for all portion of signal side and ground side respectively. Cp and Llg was calculated from these parameters by using formula (1).
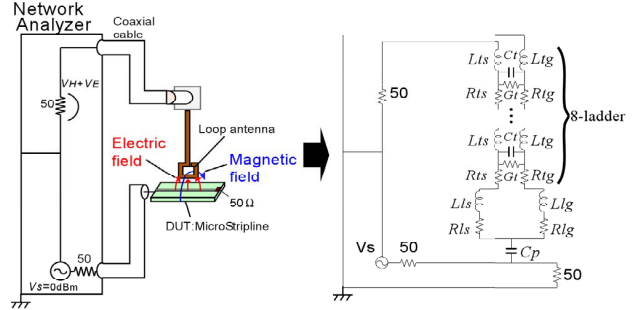

Fig. 5.   Lumped Equivalent circuit of probes including measurement setup.
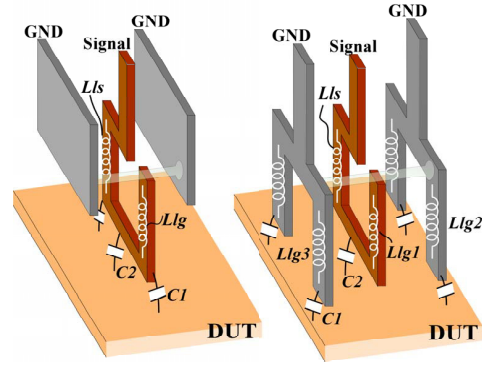

Fig. 6.   Schematic diagram for parasitic lumped parameters of loop element.

$$Cp = C1 + C2 + \cdots + Cn \qquad (1)$$
$$L\lg = L\lg 1 // L\lg 2 // \cdots // L\lg n$$

Inductances of transmission line were derived from formula (2) with signal line and ground line sectional area As, Ag and total inductance Lth was obtained by transmission line simulator. Calculated Results of those parameters is shown in table 1.

$$Ltg = Lth \cdot \frac{As}{As + 2 \cdot Ag} \qquad (2)$$
$$Lts = Lth \cdot \frac{Ag}{As + 2 \cdot Ag}$$

	Type A	Type B		Type A	Type B
Lls	0.98nH	1.8nH	Lts	0.51nH	0.44nH
Rls	0.12Ω	0.12Ω	Ltg	0.02nH	0.07nH
Llg	0.98nH	0.23nH	Ct	0.24pF	0.22pF
Rlg	0.02Ω	0.02Ω	Gt	2.7kΩ	2.9kΩ
Cp	0.021pF	0.045pF	Rts	0.12Ω	0.11Ω
			Rtg	0.004Ω	0.016Ω

Table1. Calculated value of lumped parameters

To investigate validity of equivalent circuit we estimated V_H using same circuit and same value of parameters. Fig.7 shows equivalent circuit for analysis of V_H. $Vloop$ in fig.7 means induced voltage by magnetic field and is express as $Vloop = \omega\mu SH$. Generically H applies value of magnetic field at center of loop element

(h_{center}). However, the level of magnetic field crossing through loop element doesn't have uniformity with nearing electromagnetic source more. Therefore, effective measurement height (h_{eff}) for magnetic near-field must be derived with consideration of nonuniformity inside loop. The value of h_{eff} is expressed as formula (3) in condition that integration value of uniform magnetic field inside loop is equal to that of nonuniform. In formula (3), a and b mean height of top and bottom inside loop and w is defined as distance between signal current path and return current path as shown in Fig.8.
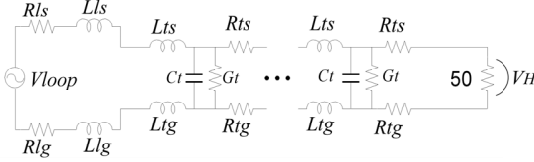

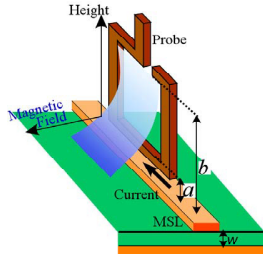Fig. 7.   Equivalent circuit of probe for evaluation of V_H induced voltage by magnetic field.

Fig. 8.   Diagrammatic illustration of magnetic field distribution inside loop element closing to target

$$h_{eff} = \frac{1}{2T}\cdot\left(-w\cdot T + \sqrt{w^2\cdot T + 4\cdot T\cdot w\cdot(b-a)}\right) \tag{3}$$

$$T = \ln\left[\frac{1}{a}\cdot(a+w)\cdot\frac{b}{b+w}\right]$$

Equivalent circuit analysis results for V_E of probe type A and B is shown in Fig.9. Resonant frequencies for type B are clearly specified and correspond with measurement result. As a result, it means that frequency characteristics for V_E including resonant frequencies can be designed with much accuracy by using the model. In high frequency band over 5GHz, theoretical results are a little higher than measurement results because those parameters in equivalent circuit don't considered frequency characteristics of dielectric constant and loss for PCB. Induced voltage by magnetic near-field V_H is as shown in Fig.10. Theoretical results conform to measurement result in all range and error was up to 3dB as shown in Fig.10. Fluctuation over 6GHz for V_H is attributed mainly to impedance miss matching around at connector or pad pattern on probe.
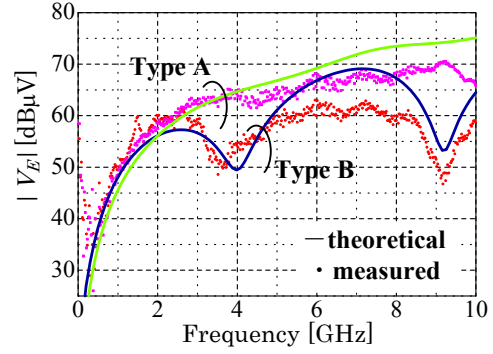

Fig. 9.   Frequency characteristics of $|V_E|$ for probe type A and type B
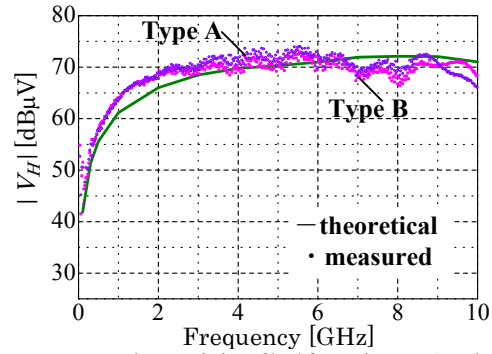

Fig. 10.   Frequency characteristics of $|V_H|$ for probe type A and type B

IV. IMPROVEMENT TECHNIQUE FOR SPATIAL RESOLUTION

To improve spatial resolution, it is necessary to lower effective measurement height h_{eff} and achieved with physical miniaturization of loop element typically [7,8]. In the meanwhile, detection range for magnetic field has trade-off with spatial resolution related to loop size and optimized probe size for each target should be fabricated and utilized respectively. However fabrication process for microscopic size tends to be complicated and miniaturized loop has further degradation of sensitivity because of stray capacitance between side and side of loop elements. Therefore we proposed measurement technique to realize variability and improvement of spatial resolution using one magnetic loop probe.
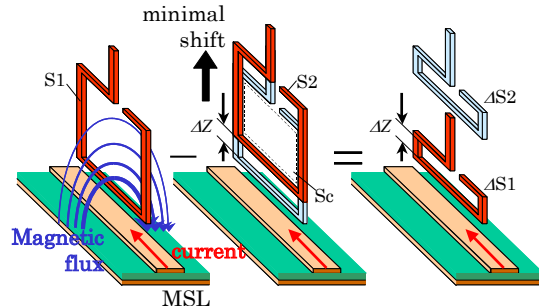

Fig. 11.   Schematic procedure of measurement for improving spatial resolution

Fig.11 shows schematic procedure of measurement to improve spatial resolution. The value of subtraction at original position and the position moved minute distance in direction of the height is measured at each measurement position. By applying the subtraction, equal resolution with an equal loop size to the distance shifted can be obtained. This simple theory is ensured by formula (4).

$$V \propto \oint_{S1} HdS - \oint_{S2} HdS$$
$$= \left(\oint_{\Delta S1} HdS + \oint_{Sc} HdS \right) - \left(\oint_{Sc} HdS + \oint_{\Delta S2} HdS \right) \quad (4)$$
$$= \oint_{\Delta S1} HdS - \oint_{\Delta S2} HdS$$

In this procedure, subtraction for top of loop should be commingling as error but can be neglected because much smaller than for the bottom part of the loop. With this technique, spatial resolution can be improved up to precision of manipulator for probe without degradation of high frequency characteristics and optimized for target respectively and easily.

Utilizing MSL as target shown in Fig.11, validity of the technique was investigated. Probe type B (1 square mm) which can suppress electric near-field in high frequency was used for magnetic probe and shifting length Δz is 30μm.
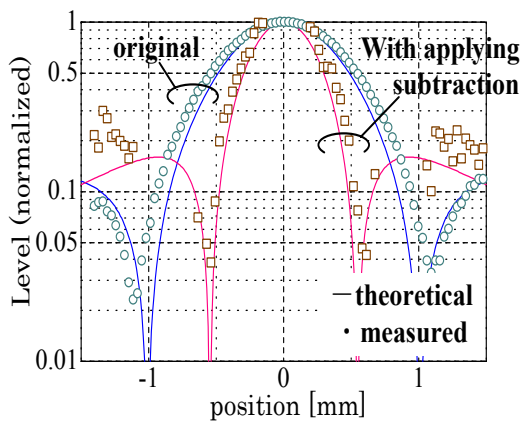

Fig. 12.   Impact of subtraction technique for improving spatial resolution

Fig.12 shows normalized measurement result of magnetic near-field distribution before and after applying the improvement technique shown as plotted. The solid lines show theoretical results, and those are calculated using simple signal and return wire current. Both of result

agreed well, and the validity of this technique and the idea was proven.

V. CONCLUSION

Magnetic near-field probe, which suppressed the influence of electrical near-field that becomes a part of reason for degradation of measurement accuracy, was fabricated.

Moreover, it was confirmed that lumped parameter equivalent circuit model including the simplified loop we proposed and the frequency characteristics of induced voltage by electric near-field and magnetic near-field were well accorded to the experimental results.

Finally, measurement method to control the spatial resolution easily by using the probe fabricated for high frequency was proposed and demonstrated. As a consequence, the measurement result conformed to the theoretical result well, and the validity of the technique was verified.

REFERENCES

[1]   K. P. Slattery, J. W. Neal, and W. Cui, "Near-field measurements of VLSI devices", *IEEE Trans. Electromagn. Compat.*, vol.41, no.4, pp.374-384, Nov. 1999

[2]   J. Shi, M. A. Cracraft, J. Zhang, R. E. DuBroff, K. Slattery, and M. Yamaguchi, "Using near-Field scanning to predict radiated Fields", *electromagnetic Compatibility 2004, International Symposium on*, Vol.1, pp.14-18, Aug. 2004

[3]   S. Kazama and K. Arai, "Adjacent electric field and magnetic field distribution measurement system", *IEEE International Symaposium on*, vol.1, 19-23, pp.395-400, Aug. 2002

[4]   E. Suzuki, S. Arakawa, H. Ota, K. Arai, R. Sato, "Optical magnetic field probe with a loop antenna element doubly loaded with electrooptic crystals", *IEEE Trans. Electromagn. Compat.*, vol.46, no.4, pp.641-647, Nov. 2004

[5]   S. Aoki, F. Amemiya, A. Kitani, N. Kuwabara, "Investigation of interferences between wireless LAN signal and disturbances from spread spectrum clocking", *electromagnetic Compatibility 2004, International Symposium on*, Vol.2, pp.505-510, Aug.2004

[6]   H. Whiteside and R. W. P. King, "The loop antenna as a probe", *IEEE Trans. Antennas Propagat.*, vol. AP-12, pp.291-297, May 1964

[7]   X Dong, S. Deng, T. Hubing and D. Beetner, "Analysis of chip-level EMI using near-field magnetic scanning", *electro-magnetic Compatibility 2004, International Symposium on*, Vol.1, pp.174-177, Aug.2004

[8]   N. Ando, N. Masuda, N. Tamaki, T. Kuriyama, S. Saito, K. Kato, K. Ohashi, M. Saito, M. Yamaguchi, "Miniaturized thin-film magnetic field probe with high spatial resolution for LSI chip measurement", *electro- magnetic Compatibility 2004, International Symposium on*, Vol.2, pp.357-362, Aug.2004